

Resonantly excited photoluminescence spectra of porous silicon

M. Rosenbauer, S. Finkbeiner, E. Bustarret,* J. Weber, and M. Stutzmann†

Max-Planck-Institut für Festkörperforschung, Heisenbergstrasse 1, 70569 Stuttgart, Germany

(Received 8 August 1994)

Resonantly excited low-temperature photoluminescence spectra of porous silicon (por-Si) samples show a steplike structure with at least four phonon-related steps. For different *n*- and *p*-doped por-Si, we examine this phonon structure in spectra taken both during laser excitation and after different detection delay times following laser shutoff, ranging from 10 μ s to 1.2 ms. The luminescence efficiency decreases and the phonon structure becomes more pronounced when lowering the excitation energy or when increasing the delay time between the detection window and the excitation. This observation suggests two separate luminescence mechanisms in por-Si: a very efficient one that is usually observed (even at room temperature) when exciting at higher energies (≈ 3 eV) and one that shows a phonon structure and can be seen only at low temperatures and when the efficient mechanism is suppressed by excitation at energies lower than 2 eV.

I. INTRODUCTION

The discovery of efficient visible red photoluminescence (PL) in porous silicon¹ (por-Si) at room temperature has not only initiated worldwide efforts in optimizing the preparation procedures for por-Si, but also challenged researchers to find the origin of this very efficient PL. Possible sources of the PL are geometrically quantum-confined electron wave functions due to quantum wires or Si nanocrystallites,¹ chemically isolated and therefore quantum-confined electron wave functions in molecular-like substances² (e.g., within a thin surface layer on top of the Si quantum wires), radiative recombination due to surface states,³ and a combination of some or all of the above mentioned effects.^{3,4}

The PL of por-Si is excited most efficiently when using photon energies in the uv or in the blue. In this case, the PL spectrum is a broadband, ranging from about 1.5 to 2.6 eV with a peak located at around 1.8 eV depending on the excitation energy. However, when exciting resonantly ($E_{\text{exc}} < 2$ eV) and at low temperatures ($T < 70$ K), the spectrum reveals a steplike structure which becomes more pronounced and eventually turns into a peak structure when reducing the excitation energy below 1.5 eV. The position of these steps or peaks relative to the excitation laser line does not change significantly when varying the excitation energy. Therefore, it is assumed that they are the manifestation of phonon structures.⁵⁻⁷ A quantitative evaluation of the step spacing energies suggests that their source must have a phonon spectrum and optical selection rules very similar to crystalline Si.⁵

The exact quantitative explanation of this phonon structure, however, is still being disputed: There is an absorption-based model⁵ by Suemoto *et al.* which assumes that the origin of the structure lies in the individual photoluminescence excitation spectra of single quantum particles. Each particle would have only one narrow emission line whose energy depends on the geometrical

size of the particle. The term resonant excitation in this model refers to exciting particles of different size and different efficiencies in their excitation spectra simultaneously with one laser line. The resulting PL spectrum would then be a superposition of the very narrow emission lines of all particles which are excited with different efficiencies. Indirect phonon-assisted absorption of these particles could explain the phonon structure. This model can also qualitatively account for the experimentally observed shift of the step onsets with increasing temperatures and for almost arbitrary numbers of steps and substeps. But both the disappearance of the steps at higher but still comparably low excitation energies and their transitions into peaks at lower excitation energies is hard to explain in this framework.

The explanation given by Calcott *et al.*^{6,7} assumes an excitonic recombination process in the indirect band structure of crystalline silicon. Phonon-assisted and non-phonon transitions account simultaneously for the optical processes and can be used to explain the step positions within experimental error. Resonant excitation in this model means selectively exciting two kinds of particles or wires, one of them having a band gap that matches the laser energy, the other one a band gap that is below the laser energy by exactly the energy of one crystalline silicon phonon at a Δ point in \vec{k} space (e.g., by the energy of a TO phonon being 57 meV). After a fast relaxation into triplet states, the excited states of both kinds of quantum wires could decay directly or by emitting a Δ phonon. Therefore, this model can only explain exactly three steps in the spectrum: the zero-, the one-, and the two-phonon step. It was shown theoretically⁸ that the phonon-assisted transitions should have a 3-10 times higher oscillator strength than the zero-phonon transitions. Temperature effects on the step structure are not discussed.

In this paper, we present experimental results concerning the phonon structure and examine whether this struc-

ture is an intrinsic effect of the efficient luminescence in por-Si and can therefore be used to settle the questions concerning the basic PL mechanisms in por-Si. Since the phonon structure only occurs at low excitation energies and with very low quantum efficiency, it seems likely that it is caused by a different PL mechanism which only becomes visible when it is not covered by the much more efficient usual luminescence in por-Si.

II. EXPERIMENT

We have investigated two types of por-Si samples: samples made of *n*-type Si wafers (P doped, 1.5 Ω cm), which had been etched with 50 mA/cm² for 10 min, and samples made of *p*-type Si wafers (\approx 20 Ω cm) of 80% porosity, etched with about 20 mA/cm² anodization current. In this text, we are referring to these samples as *n* type and *p* type. For comparison, we have also measured anodized amorphous silicon obtained from a 2- μ m-thick boron-doped layer of hydrogenated amorphous silicon. Details of the preparation of this anodized *a*-Si:B:H sample are given in Ref. 9. All samples were stored in air for more than 1 yr and showed a bright orange luminescence visible to the naked eye when illuminated by a weak uv lamp at room temperature (quantum efficiency of the por-Si samples was about 10%).

In order to obtain a free-standing film of the *n*-type sample for the optical absorption measurements, we removed the top SiO₂ layer with hydrofluoric acid and then put a transparent self-adhesive tape onto the surface. When removing the tape, a closed free-standing film of about 40 μ m thickness stuck to the tape, which showed bright orange luminescence when illuminated from either side by a weak uv lamp. The remaining substrate showed the luminescence too. The absorption coefficient was measured by photothermal deflection spectroscopy¹⁰ (PDS); the signal was corrected for the absorption of the adhesive tape. Immediately after the absorption measurement, the PL activity of the layer was unchanged. A few days later, however, it had disappeared. Then the absorption of the layer was measured again.

For excitation of the PL spectra, Kr⁺, HeNe, and Ti:Al₂O₃ lasers were used. The blue part of the PL excitation measurements was taken using a xenon arc lamp with a monochromator. Usually, the excitation power was around 300 mW/cm². The detection system was either an optical multichannel analyzer system with a gated light intensifier stage and a single monochromator or a gated photomultiplier system with a double monochromator. All spectra were corrected with respect to the particular system response. In this paper, we show both spectra that were taken during cw laser excitation (cw spectra) and time-delayed spectra where the laser beam was chopped with 100 Hz with an on-off ratio of 1:2 and the spectrum was recorded starting a delay time *T* after laser shutoff. Typical delay times were 10 μ s, 200 μ s, and 1.2 ms with detection windows of 200 μ s, 1000 μ s, and 4200 μ s, respectively.

III. RESULTS

A. General

Figure 1 shows typical PL spectra of a por-Si sample which is excited resonantly. The room temperature spectrum shows a PL at energies above the excitation energy, the anti-Stokes tail. The low-temperature PL spectrum, on the other hand, starts with a sharp onset about 6 meV below the the laser energy. It shows a steplike phonon structure.

The PL spectra of por-Si are excited most efficiently when using photon energies between 2 and 5 eV (see Figs. 2 and 3). Further lowering the excitation energies results in a rapidly decreasing quantum yield. The optical absorption (determined by PDS) of a self-supporting por-Si film obtained from the same sample, however, does not show a decrease of the same order of magnitude (see Figs. 2 and 4). For comparison, we have included the results published by other groups in Fig. 4. In contrast to the results in Ref. 11, the data in Fig. 4 are not corrected for the porosities of the samples and thus show an effective macroscopic absorption coefficient α_{eff} . Note that the results published by different groups and obtained from different samples can vary by more than one order of magnitude. Therefore it is important to correct the PL excitation spectra by the absorption coefficient measured on the same sample.

B. PL excited at different energies

When varying the excitation energy, the peak of the PL spectrum is shifted too. As can be seen in Fig. 3, there is a Stokes shift of more than 2 eV between the laser line and the PL maximum when exciting above 4 eV. When exciting at energies below 2.1 eV, the peak of the PL spectra stays almost constant (between 1.5 and 1.6 eV) and the Stokes shift decreases to values below 0.2 eV. At

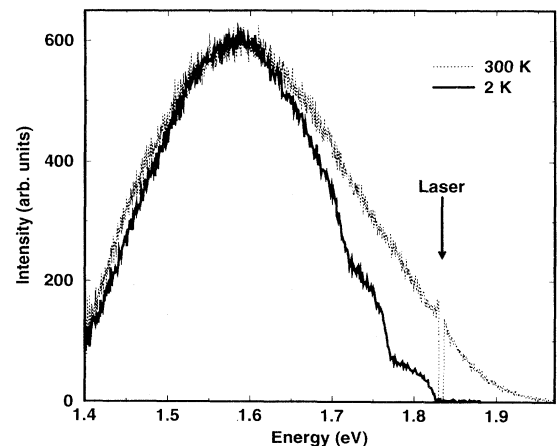


FIG. 1. Typical luminescence spectra of por-Si under resonant excitation (1.833 eV) at room temperature and at 2 K.

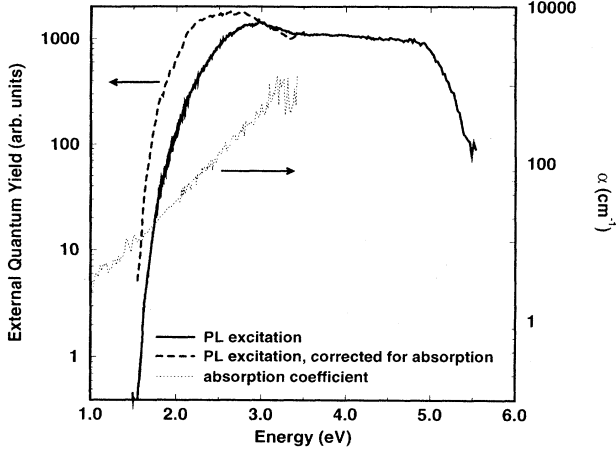


FIG. 2. Low-temperature photoluminescence excitation spectrum of the n -type sample. The detector was scanning from 2.1 to 1.4 eV simultaneously with the excitation source and always detecting the peak of the luminescence. Since the thin por-Si layer becomes increasingly transparent when lowering the excitation energy (compare the absorption coefficient plotted in this graph; see also Fig. 4), we show with the dashed line a PL excitation spectrum that is corrected for this effect.

the same time, the PL efficiency goes down by orders of magnitude, as shown in Fig. 2, and the step structure becomes visible. The lower the overall PL intensity, the more pronounced the steps become. In Fig. 3, the spectra were scaled according to their peak quantum efficiency. There is always PL between 1.4 and 1.8 eV, no matter what particular energy was used for excitation.

In Fig. 2, we show the excitation spectrum obtained from the n -type sample. Since the peak position of the PL spectra depends on the excitation energy (see Fig. 3),

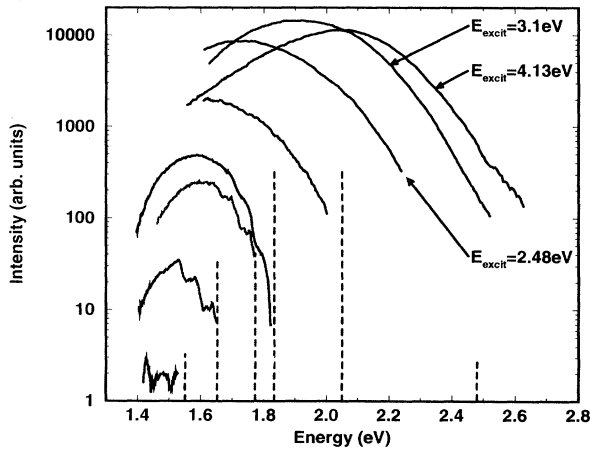


FIG. 3. Low-temperature PL spectra of n -type por-Si without delay. The spectra were scaled according to their quantum efficiency determined from PL excitation measurements at the same temperature (see Fig. 2). The excitation energies are marked by straight lines and are labeled.

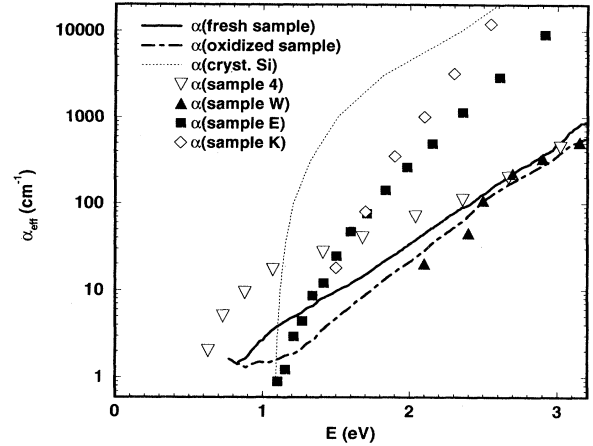


FIG. 4. Effective absorption coefficient (not corrected for porosity) of a free-standing por-Si film obtained at room temperature from the n -type sample using PDS (see Sec. II). The dashed line is a measurement taken from the same film a few days later when it did not luminesce any more. For comparison, we also plot the absorption coefficient of crystalline Si and the results from Ref. 21 (sample 4), Ref. 22 (sample W), and Ref. 3 (sample K) and show the results obtained from a p -doped sample with 70% porosity (sample E). The Urbach energies for the different samples (defined by $E_0 = \frac{\partial \hbar\omega}{\partial \ln(\alpha)}$) are as follows: fresh sample, 400 meV; oxidized sample, 340 meV; sample 4, 600 meV; sample W, 420 meV; sample E, 260 meV; sample K, 180 meV.

we moved both the detector and the excitation source simultaneously. The PL excitation spectrum shows that the PL in our por-Si samples is excited most efficiently by laser energies between 2.5 and 5 eV. At lower energies, the porous layer is penetrated by the excitation light and most of the light is absorbed in the Si substrate. Therefore one has to correct the external quantum yield for the energy-dependent absorption of the porous layer. The corrected quantum yield is shown in the PL excitation spectrum (Fig. 2) as a dashed line.

The phonon steps can also be detected in the PL excitation spectra. As the laser is scanned, different parts of the PL spectrum appear at the detection energy. Figure 5 shows an example of such a PL excitation spectrum, which was detected at $E = 1.512$ eV. Since the PL is excited more efficiently at higher energies, this spectrum covers more than two orders of magnitude in PL intensity. The lower part of Fig. 5 shows the second derivative of the PL excitation spectrum in order to accentuate the position of the steps (see Sec. III E).

C. Anti-Stokes tail

When exciting resonantly, we find a luminescent tail on the high-energy (anti-Stokes) side of the laser at room temperature (see Fig. 1). This tail can be described by

$$I(E) \propto e^{-(E-E_{exc})/(ak_B T)} \quad (3.1)$$

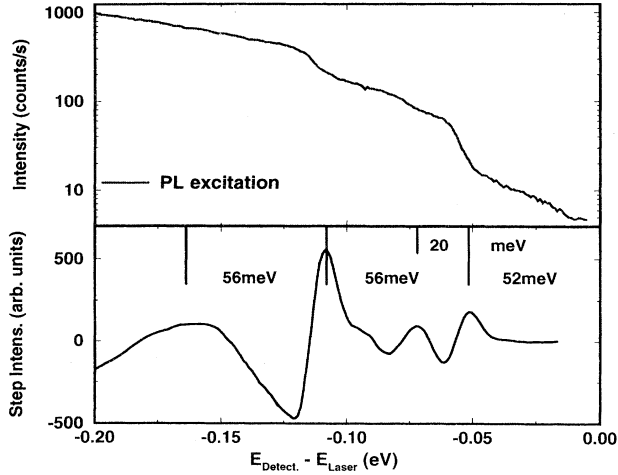


FIG. 5. Upper part: phonon structure observed in PL excitation at 15 K. The detector was at 1.512 eV and the laser power was about 300 mW/cm². Lower part: second derivative of the graph above.

for all temperatures between 400 K and 20 K (see Fig. 6). I is the luminescence intensity, E the detection energy, E_{excit} the laser energy, k_B the Boltzmann constant, T the sample temperature, and a a constant that is larger than 1. In most of our measurements, we find values around $a = 1.4 \pm 0.1$. There is no difference between time-delayed and cw measurements.

D. PL close to the energy of the laser line

As can be seen in Fig. 1, the high-energy side of the PL spectrum changes when reducing the sample temperature from room temperature to 2 K. The anti-Stokes tail dis-

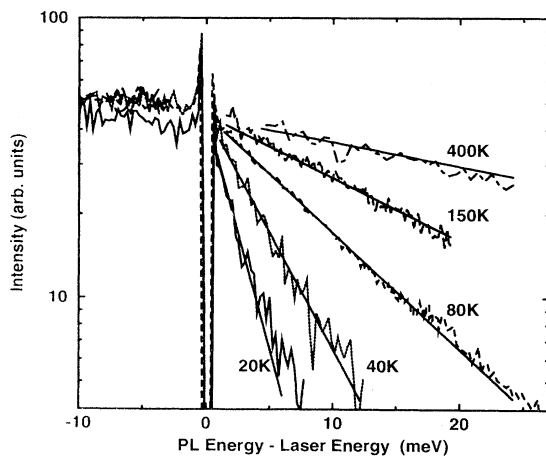


FIG. 6. PL spectrum of the *n*-type por-Si sample on the high-energy side of the laser line (anti-Stokes tail) at different temperatures. The straight lines are fits according to Eq. (3.1). $E_{\text{excit}} = 1.833$ eV, $a = 1.5$.

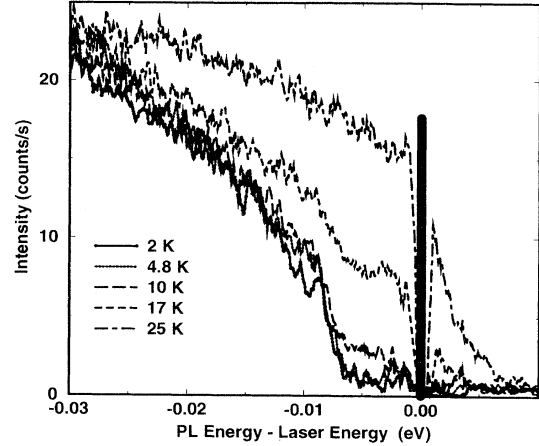


FIG. 7. PL spectrum of the *n*-type por-Si sample at the low-energy side of the laser line (1.833 eV). The spectral gap of about 6 meV is filled at temperatures as low as 20 K. At the same temperature, one can see the anti-Stokes tail.

appears completely and on the Stokes side, the spectrum is narrower and shows the phonon structure reported in Refs. 5–7. Furthermore, the onset of the PL spectrum is about 6 meV below the laser line. Figure 7 shows how the shape of the PL spectrum changes when raising the sample temperature up to 25 K: the gap in the spectrum between the 2 K PL onset and the laser line is filled at low temperatures and disappears at temperatures above $T = 20$ K. We calculate the activation energy for the luminescent states in this spectral gap for temperatures between 4 and 25 K (see Fig. 8). This activation energy of around 1 meV is considerably lower than the width of the spectral gap itself.

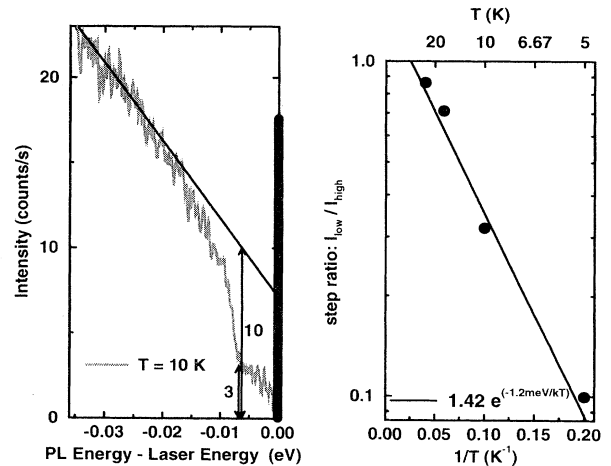


FIG. 8. The fraction of luminescent states within the spectral gap (see Fig. 7) is determined as shown in the left part of the figure. The values thus obtained lie on a straight line in an Arrhenius plot. The activation energy of these luminescent states is determined from its slope.

E. Step onset energies

On the low-energy side of the laser, we find the previously reported steps in the PL spectrum. In all samples, there are at least four steps (including the zero-phonon step directly at the laser energy) with an energy distance of 56 ± 1 meV between each step, starting about 6 meV below the laser energy at low temperatures. In order to determine these step onset energies more precisely, we plotted the second derivative of the smoothed spectra. As indicated in Fig. 9, the second derivative shows four clearly visible maxima exactly at the positions of the onsets of the steps. A numerical check shows that there is no significant shift of the thus obtained step onset energies due to the curvature of the underlying main luminescence peak.

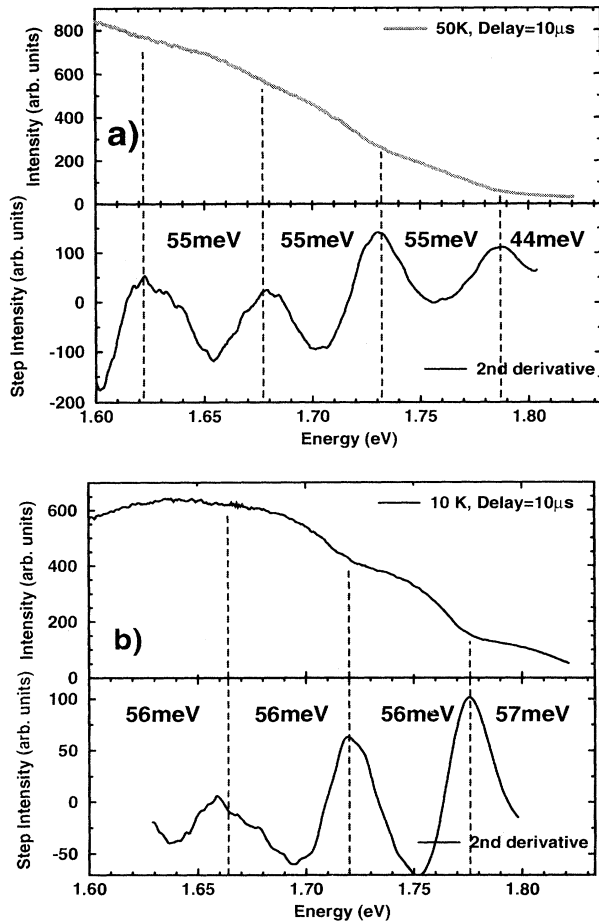


FIG. 9. Upper part: PL spectra of (a) the *n*-type sample at 50 K and (b) the *p*-type sample at 10 K, taken with a delay of 10 μs and an excitation energy of 1.833 eV. Lower part: the second derivative of the smoothed spectrum has maxima at the step onset positions of the spectrum. Within experimental error, these step onset positions have a constant distance of about 56 meV. Note that the first onset energies (44 meV and 57 meV) are different from 56 meV because of the spectral gap close to the laser and the temperature-dependent shift of the phonon structure towards the laser (see Fig. 11).

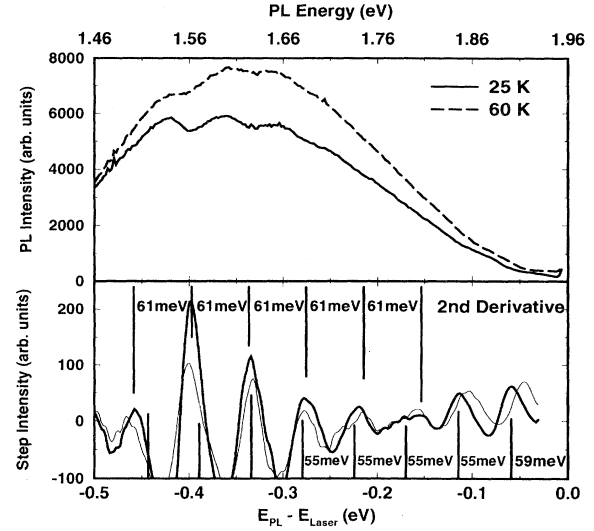


FIG. 10. Upper part: PL spectrum of the *n*-type sample at different temperatures, cw excited at 1.960 eV. Lower part: second derivative of the smoothed spectra. The step onset energies in the high-energy part are dominated by the temperature-dependent phonon structure with a period of 55 meV, whereas the low-energy regime is dominated by the PL fine structure (see also Fig. 13) with a periodicity of 61 meV.

Comparing PL spectra taken at different temperatures, we find a monotonically increasing shift of the onset energies of the zero-, one-, two-, and three-phonon transitions towards higher energies with increasing temperature, as can be seen in Fig. 10 (one-, two-, and three-phonon transition) and is illustrated in Fig. 11. This observation is consistent with both the filling of the spectral gap and the

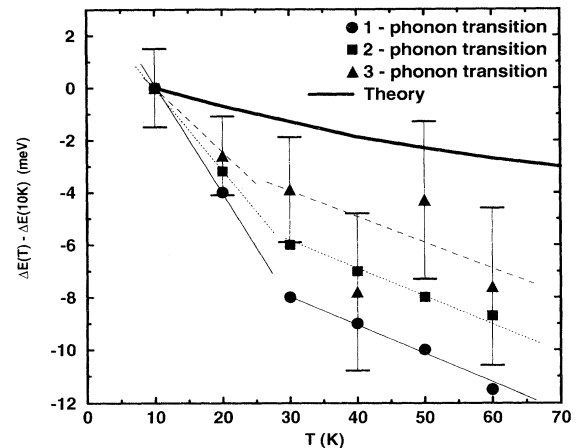


FIG. 11. Shift of the step onset energies with respect to their position at 10 K. At this temperature, absolute step onset energies E_0 are $E_{laser} - 57$ meV, $E_{laser} - 112$ meV, and $E_{laser} - 172$ meV for the one-, two-, and three-phonon transitions, respectively. The spectra were taken with the *p*-type por-Si sample with a delay time of 25 μs and a detection window of 500 μs. The solid line is the expected shift of the step onset energies according to the theory outlined in Ref. 5.

anti-Stokes tail mentioned above. The filling of the spectral gap occurs at temperatures below 20 K and explains the high slope in this region in Fig. 11. At temperatures above 20 K, the exponential tail at the anti-Stokes side of the laser builds up and has a counterpart at each of the steps causing their apparent onset energies to shift towards the blue. This explains the low-slope region of Fig. 11 above $T = 30$ K.

F. Fine structure

In some cases, we were able to see a different structure, the so-called fine structure of the PL spectrum in our samples. It has already been observed several times and is described in Refs. 12–15. Its origin is still unknown, but interference effects can be ruled out.¹⁵ We find that it can be present both when exciting resonantly and when exciting with blue laser lines. It does not make a difference whether the spectra are taken continuously or time delayed. Figure 10 shows a superposition of the phonon structure with the fine structure. The periodicity of the fine structure and the phonon structure is different. Note that the fine-structure peak spacing of 60 ± 1 meV is close to the maximum in the phonon density of states (DOS) of crystalline Si (61 meV) or amorphous Si (59 meV). The 50 K spectrum in Fig. 12(b) also shows the fine structure. We find neither a temperature dependence nor a dependence on the excitation energy of the fine structure peak positions. In addition, they are the same for all samples as illustrated in Fig. 13. This fine structure can only be seen under certain conditions, which we cannot reproduce completely. Temperatures between 10 and 60 K seem to be favorable as well as a long precooling

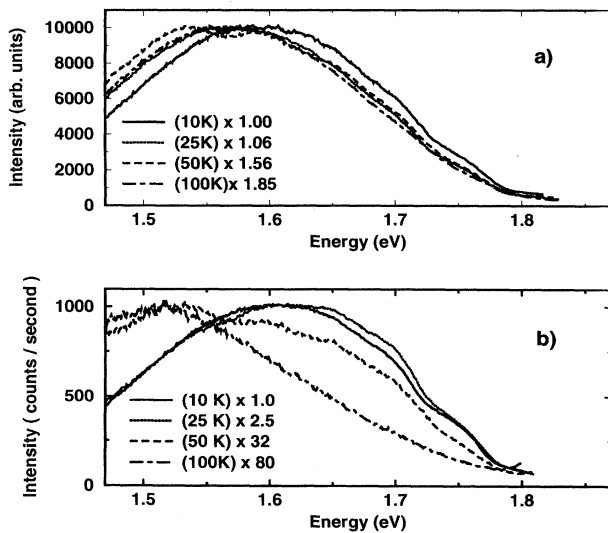


FIG. 12. Normalized PL spectra at different temperatures. The scaling factors are given in the legends. The spectra in (a) are taken after $10 \mu\text{s}$ delay with a time window of $200 \mu\text{s}$. The spectra in (b) are taken after 1.2 ms delay with a window of 3 ms. The excitation energy is 1.833 eV.

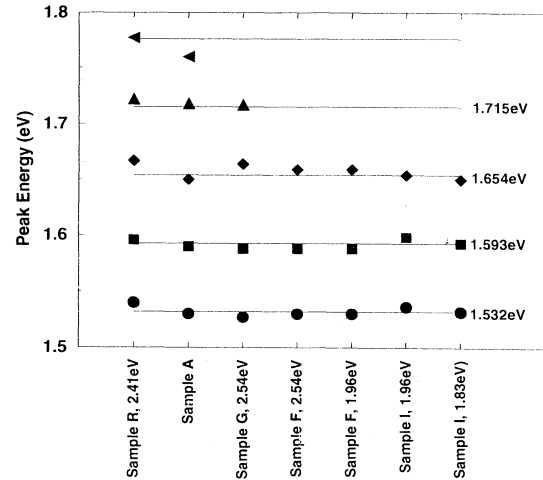


FIG. 13. Energies of the fine-structure peaks taken from various samples. The results for sample *R* are extracted from Ref. 14 and the results for sample *A* from Ref. 12; samples *F* and *G* are *p*-type samples and sample *I* is *n* type. The energies given with the samples denote the excitation energies. The horizontal lines have a constant distance of 61 meV. The fine structure is only present in the spectra of the samples under certain conditions (see Ref. 15).

time of the sample in the cryostat. Cycling the temperature between helium and room temperature causes the effect to disappear. One of the authors has seen the fine structure even at room temperature using grazing angle incidence for excitation.

The origin of the fine structure is even less clear than the mechanism of the efficient room temperature PL in por-Si and has been subject to discussions in the literature, e.g., in Ref. 15. Residues from the chemicals used for etching the por-Si samples might play a role.

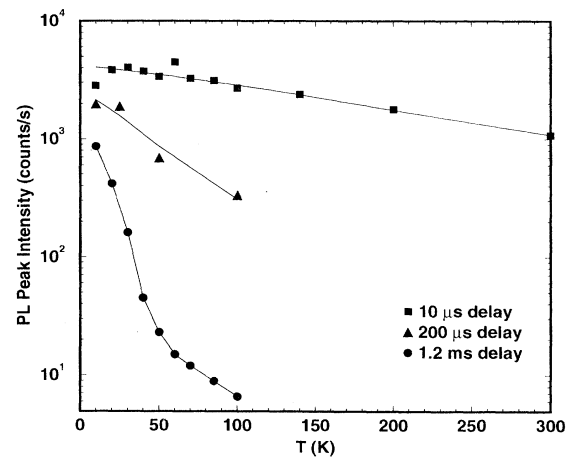


FIG. 14. Temperature dependence of the PL intensity of the *n*-type sample at different delay times.

G. PL dependence on temperature and delay time

The temperature dependence of the PL spectra shown in Fig. 14 is different at long delay times from short times after laser shutoff. Figure 10 shows how a PL spectrum (taken in the cw mode) depends on the sample temperature. When raising the temperature from 25 to 60 K, the overall luminescence intensity increases and simultaneously all steps become less pronounced. A similar behavior can be found in Fig. 12. Figure 12(a) shows PL spectra taken 10 μ s after excitation and the spectra in Fig. 12(b) are taken 1.2 ms after excitation. All spectra are scaled to the same maximum intensity; the scaling factors are presented in the legends. In Fig. 12(b), the steps can be seen more clearly than in Fig. 12(a), although the PL intensity after 1.2 ms is considerably weaker than at short delay times.

IV. DISCUSSION

Summarizing the results, we find efficient PL and spectra which show one broad structureless peak with an energy between 1.6 and 2.0 eV when exciting at energies above 2 eV (see Figs. 2 and 3). When reducing the excitation energies from 2 eV to about 1.6 eV, the luminescence efficiency (even when corrected for varying optical absorption) decreases by more than two orders of magnitude and features such as the phonon structure or the anti-Stokes tail become visible. Also, for a fixed excitation energy, when looking at longer delay times (e.g., in Fig. 12 with a delay of more than 1 ms), the luminescence intensity decreases by more than one order of magnitude when compared to a delay of 10 μ s, but the low-temperature phonon steps can be seen more clearly [comparing Fig. 12(a) with Fig. 12(b)]. The steps are not scaled down with the same scaling factor as the overall luminescence background. Therefore the steps seem to be caused by a process with a slightly longer decay time, which would be expected, e.g., for indirect transitions.

One way to explain these observations is to assume that there are two processes which simultaneously cause the low-temperature luminescence in por-Si. Process I is the known, very efficient process, which is mainly invoked by excitation above 2 eV and which is present at all temperatures up to room temperature. It has a Stokes shift of 0.4–2 eV and its light emission covers a wide energy range, which always contains the energies between 1.4 and 2 eV (see Figs. 3 and 1). The other process, process II, can only be detected when it is not hidden under the much brighter usual luminescence of the same energy. It can be seen most clearly when exciting at energies below 1.8 eV or when exciting at slightly higher energies and looking after a long delay time, i.e., when the usual luminescence is suppressed. At low temperatures, it shows a phonon structure with more than three steps (including the zero-phonon transition) which are separated by a constant difference in energy of 56 ± 1 meV.

To find out which of these two processes is related to

crystalline silicon as the luminescent agent, we recorded the PL spectra of a sample made out of amorphous silicon (anodized *a*-Si:B:H): Fig. 15(a) shows that the spectra of por-Si and anodized *a*-Si:B:H obtained at room temperature under uv excitation are similar, whereas the spectra obtained at He temperature by excitation below 2 eV [Fig. 15(b)] are completely different. The anodized *a*-Si:B:H sample does not show any phonon structure or a spectral gap. Apparently process II, which accounts for the luminescence of por-Si when excited below 2 eV, is not present in this sample. The peak of the PL spectrum has a much smaller Stokes shift (only ≈ 35 meV) and can be interpreted as the low-energy tail of process I. Therefore we conclude as a first major result of this work that the weak low-energy PL of porous Si, which exhibits the phonon structure (process II), most likely constitutes a separate radiative process linked to the crystalline Si skeleton, but is not directly connected to the strong process I giving rise to the visible luminescence at room temperature.

Next we discuss the possible origin of the phonon structure in process II. The first three phonon steps in the PL spectra are predicted correctly by the model of Calcott *et al.* as described in the Introduction. The detection of more than three steps in the phonon structure (see Fig. 9) remains unexplained as well as the fact that the phonon substeps (see Figs. 5 and 3) are visible only when exciting below 1.8 eV. On the other hand, as summarized in Table I, the observed characteristic phonon energy of 56 ± 1 meV is best explained via \vec{k} -conserving TO(Δ) phonons in crystalline Si.

The model of Calcott *et al.*^{6,7} does not discuss any effects of elevated temperatures. Suemoto *et al.*,⁵ on the other hand, include influences of the temperature T on the absorption coefficient in two ways. First, the absorp-

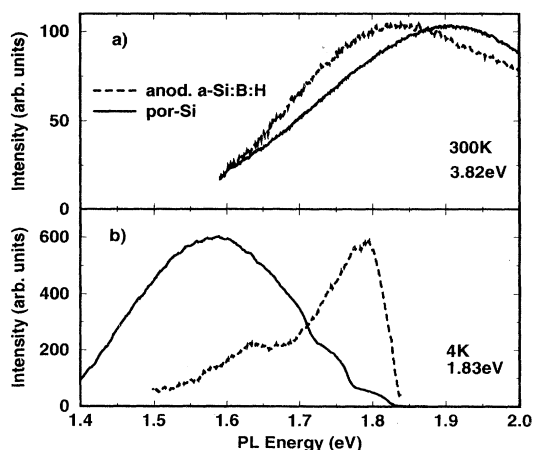


FIG. 15. PL spectra of partially oxidized amorphous silicon (anodized *a*-Si:B:H) and *n*-type por-Si. The spectra are normalized. The anodized *a*-Si:B:H sample is luminescing less efficiently than the por-Si sample by about one order of magnitude. (a) shows room temperature PL spectra excited in the uv and the spectra in (b) are measured at He temperature under resonant excitation.

TABLE I. List of phonon energies possibly related to the fine structure or to the phonon structure in por-Si.

Energy (meV)	Reference	Assignment
65	23	maximum phonon energy in crystalline Si
61	23	maximum phonon DOS in bulk Si
61±1		experimentally determined fine-structure periodicity
59±1	24	maximum phonon DOS in <i>a</i> -Si:H depending on hydrogen content
57.3	25	TO(Δ) phonon in crystalline Si
56±1		experimentally determined periodicity of phonon structure
55.3	25	LO(Δ) phonon in crystalline Si
20		experimentally determined energy shift of the phonon substeps
20	24	local maximum phonon DOS in <i>a</i> -Si:H
18.2	25	TA(Δ) phonon in crystalline Si

tion of every single luminescent particle is affected by T via the Bose factor. This has almost no effect on the step onset energies. Second, thermal excitation can cause particles to emit at higher energies than their ground state energy. Therefore, a whole ensemble of particles of different sizes can emit at a certain detection energy with a probability which depends on the amount of thermal excitation (Boltzmann-distributed) necessary to match the detection energy.

In order to compare our results with the predictions of this latter model, we calculated the spectra and the absorption coefficients for temperatures between 10 and 80 K using the distribution function and the fit parameters from Ref. 5. We always used formula (5) in Ref. 5, even for low temperatures. Then we smoothed these spectra and calculated the second derivative using the same algorithm as used for our experimental data. The results for the shift of the step onset energies are shown in Fig. 11. Their temperature dependence is weaker than the experimental one. The main difference between the experimental data and the expected temperature dependence is due to the disappearance of the spectral gap directly at the laser line between 2 and 30 K (cf. Fig. 7). Based on our experimental results in Figs. 6, 7, and 11, we suggest the following explanation for the temperature dependence of the phonon structure. At finite temperatures, occupied states both at the laser energy and at lower energies are further excited thermally and give rise to the exponential anti-Stokes tail on the high-energy side of the laser as well as to similar shifts of the step onsets on the low-energy side.

Independent measurements with optically detected magnetic resonance have shown that the light emitting transition in por-Si originates from a well-defined triplet state.¹⁶ In this context, the assumption of an enhanced exchange splitting (≤ 6 meV) of localized excitons, outlined in Ref. 7, seems to be reasonable and explains the presence of the spectral gap shown in Fig. 7: the upper state, the singlet state, was excited and either decays immediately or relaxes to a longer lived triplet state that

is at least 6 meV below the singlet state. This is further confirmed by independent measurements¹⁷ of the lifetime of the luminescent states at 1.6 eV, which show a jump from 10 ms at 10 K to about 200 μ s at $T > 60$ K. The behavior of this spectral gap around 20 K, however, is not easily explained by this theory. If there are states that start to decay radiatively after activation by thermal energies as low as 1 meV (see Sec. III D), they can only be explained by assuming pairs of states within the spectral gap which are split by about 1 meV and for which the radiative transitions from their lower levels are forbidden. In contrast to the aforementioned triplet states, radiative transitions out of these states do not occur at temperatures below 5 K.

As described above, there is a difference in the luminescence properties of por-Si when excited above or below about 2 eV: when switching from process I to process II (see above) by reducing the excitation energies towards 1.6 eV, the photoluminescence efficiency decreases rapidly and the step structure becomes visible. The absorption coefficient α of the por-Si layer, however, follows the same exponential law

$$\alpha(E) \propto e^{E/E_0} \quad (4.1)$$

with $E_0 = 404$ meV for E ranging from 0.8 to 3.2 meV and does not show any features around 2 eV (see Fig. 4). It follows that the change of the PL properties at 2 eV only affects the radiative and nonradiative recombination mechanisms and not the absorption. It is particularly interesting to note that the absorption spectra show only little changes upon aging. There is only a slight decrease of the band gap due to oxidation, whereas the PL decreases by more than two orders of magnitude. This shows that there is no direct relation between PL and absorption in por-Si. The PL quenching due to the slow room temperature oxidation can be understood by comparing with well-investigated effects of thermally oxidizing porous silicon at temperatures between 200 °C and 600 °C.^{18,19} There it was concluded that dangling bonds,

which act as efficient noradiative recombination centers and thus quench the luminescence, occur as a consequence of incomplete oxidation of a previously hydrogen-terminated inner surface. The anticorrelation between electron spin resonance spin density and luminescence intensity at 300 K has been shown, e.g., in Ref. 20. In the PDS spectra of Fig. 4, the defect absorption of these 10^{17} – 10^{18} defects cannot be seen due to the strong absorption of suboxide band tail states.

V. CONCLUSION

Our experimental results show that none of the existing theories can explain all experimental aspects of the phonon structure in the PL of por-Si. Some of our measurements can be explained only by assuming two separate luminescence mechanisms in por-Si: one that is

efficient and dominates the PL spectra when exciting at energies above 2 eV and one that shows a phonon structure and can only be seen when the first one is suppressed. Only the efficient luminescence mechanism can be seen at room temperature. The attempt to take the phonon structure as a proof for crystalline silicon being the source of the luminescence in por-Si (as done in Ref. 6) therefore only concerns the weaker PL mechanism.

ACKNOWLEDGMENTS

We thank H. Hirt, P. Wurster, and M. Siemers for technical support. This work was supported by the European Union under PECO Project No. 7839. We also thank W. Lang, P. Steiner, and L.T. Canham for supplying samples.

* Permanent address: Laboratoire d'Etudes des Propriétés Electroniques des Solides, CNRS, 166X, F-38042 Grenoble, France.

† Permanent address: Walter-Schottky-Institut, Technische Universität München, Am Coulombwall, D-85748 Garching, Germany.

¹ L.T. Canham, *Appl. Phys. Lett.* **57**, 1046 (1990).

² P. Deák, M. Rosenbauer, M. Stutzmann, J. Weber, and M. Brandt, *Phys. Rev. Lett.* **69**, 2531 (1992).

³ F. Koch, V. Petrova-Koch, T. Muschik, A. Nikolov, and V. Gavrilenko, in *Microcrystalline Semiconductors: Materials Science & Devices*, edited by P.M. Fauchet *et al.*, MRS Symposia Proceedings No. 283 (Materials Research Society, Pittsburgh, 1993), p. 197.

⁴ F. Buda, J. Kohanoff, and M. Parinello, *Phys. Rev. Lett.* **57**, 1272 (1992).

⁵ T. Suemoto, K. Tanaka, A. Nakajima, and T. Itakura, *Phys. Rev. Lett.* **70**, 3659 (1993).

⁶ P.D.J. Calcott, K.J. Nash, L.T. Canham, M.J. Kane, and D. Brumhead, in *Microcrystalline Semiconductors: Materials Science & Devices* (Ref. 3), p. 143.

⁷ P.D.J. Calcott, K.J. Nash, L.T. Canham, M.J. Kane, and D. Brumhead, *J. Phys. Condens. Matter* **5**, L91 (1993).

⁸ M.S. Hybertsen, *Phys. Rev. Lett.* **72**, 1514 (1994).

⁹ E. Bustarret, M. Ligeon, and L. Ortéga, *Solid State Commun.* **83**, 461 (1992).

¹⁰ W.B. Jackson, N.M. Amer, A.C. Boccara, and D. Fournier, *Appl. Opt.* **20**, 1333 (1981).

¹¹ I. Sagnes, A. Halimaoui, G. Vincent, and P.A. Badoz, *Appl. Phys. Lett.* **62**, 1155 (1993).

¹² N.S. Averkiev, V.M. Asnin, I.I. Markov, A.Yu. Silov, V.I. Stepanov, A.B. Churilov, and N.E. Mokrousov, *Pis'ma*

Zh. Eksp. Teor. Fiz. **50**, 631 (1992) [*JETP Lett.* **55**, 657 (1992)].

¹³ V.M. Asnin, N.S. Averkiev, A.B. Churilov, I.I. Markov, N.E. Mokrousov, A.Yu. Silov, and V.I. Stepanov, *Solid State Commun.* **87**, 817 (1993).

¹⁴ G.W. 't Hooft, Y.A.R.R. Kessener, G.L.J.A. Rikken, and A.H.J. Venhuizen, *Appl. Phys. Lett.* **61**, 2344 (1992).

¹⁵ M. Rosenbauer, H. Fuchs, and M. Stutzmann, *Appl. Phys. Lett.* **63**, 565 (1993).

¹⁶ M. Stutzmann, M.S. Brandt, M. Rosenbauer, H.D. Fuchs, S. Finkbeiner, J. Weber, and P. Deak, *J. Lumin.* **57**, 321 (1993).

¹⁷ S. Finkbeiner and J. Weber, *Thin Solid Films* **255**, 254 (1995).

¹⁸ L. Tsybeskov and P.M. Fauchet, *Appl. Phys. Lett.* **64**, 1983 (1994).

¹⁹ K.-H. Li, C. Tsai, J.C. Campbell, B.K. Hance, and J.M. White, *Appl. Phys. Lett.* **62**, 3501 (1993).

²⁰ B.K. Meyer, V. Petrova-Koch, T. Muschik, H. Linke, P. Omling, and V. Lehmann, *Appl. Phys. Lett.* **63**, 1930 (1993).

²¹ V. Grivickas and P. Basmaji, *Thin Solid Films* **235**, 234 (1993).

²² L. Wang, M.T. Wilson, and N.M. Haegel, *Appl. Phys. Lett.* **62**, 1113 (1993).

²³ *Phonon Dispersion Relations in Insulators*, edited by H. Bilz and W. Kress (Springer-Verlag, Berlin, 1979), p. 97.

²⁴ W.A. Kamitakahara, H.R. Shanks, J.F. McClelland, U. Buchenau, F. Gompf, and L. Pintschovius, *Phys. Rev. Lett.* **52**, 644 (1984).

²⁵ K.L. Shaklee and R.E. Nahory, *Phys. Rev. Lett.* **24**, 942 (1970).